Supplementary Figure Legends

Figure S1. Gradient conditions for the chromatographic methods used in this study. The gradients for the RPLC- (A) and HILIC-based (B) analysis. See methods for a complete description of these conditions. For RPLC, solvent B consists of 10mM ammonium formate in methanol; solvent A consists of 10mM ammonium formate in water. For HILIC, solvent B consists of 90% acetonitrile with 15 mM ammonium formate; solvent A is composed of 10 % acetonitrile with 15 mM ammonium formate.

Figure S2. Diet alters the taxonomic distribution in the humanized mouse microbiota. Values represent the average relative abundance across all samples within a group for the RD (n= 3) or PDD (n=3) fed mice. Significant differences between samples ($p<0.05$) are indicated with an asterisk.

Figure S3. Urinary metabolomic profile of humanized mice clusters by diet. PCA plot of urine metabolite profiling from humanized mice fed RD (n= 3) or PDD (n=3).

Figure S4. Simplified model microbiotas alter urine metabolome. Heat-map of microbe-dependent metabolites from urine samples of gnotobiotic mice colonized with *Bacteroides thetaiotaomicron* (BT)*, Bt* and *Bifidobacterium longum* (BTBL) or humanized mice (HUM). Left panel (A) shows features significantly detected in samples of gnotobiotic mice. Right panel (B) shows GF-related features that significantly decrease in the presence of gut microbiota. Fold-changes are relative to the respective metabolomes of GF animals. Significance is defined by fold change>10 and p value< 0.01. m/z values in red indicate GF related features that disappear in all colonization states.

Figure S5. Indolelactic acid production by *Bl.* A. LC-MS spectrum (ESI Positive mode) that shows production of indolelactic acid by *Bl in vitro* (middle) relative to starting medium (top) and an indolelactic acid standard (bottom). B. MS/MS spectrum that confirms the identity of indolelactic acid based on fragmentation ions.

Figure S6. Metabolomes of one and two member model microbiotas do not reconstitute the metabolomic complexity of a humanized microbiota. Venn diagram of microbe-dependent metabolites from fecal samples of gnotobiotic mice colonized with *Bacteroides thetaiotaomicron* (BT), *BT* and *Bifidobacterium longum* (*BTBL*) or humanized mice (HUM). These features are significantly different from germ free mice fecal metabolites; defined by fold change>10 and p value< 0.01 .

Figure S7. Humanized mice reproduce some aspect of human fecal metabolome. RPLC-ESI+ spectra of two features specific to donor 3 and the respective recipient mice.

Figure S8. Structures of identified compounds. Chemical structures of verified compounds (see Table S2) and exact masses.

A.

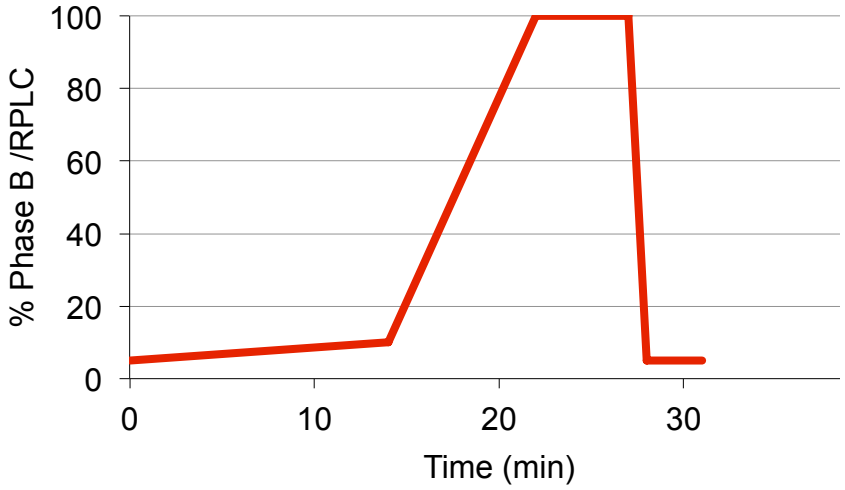
100
80
60
40
20
0
% Phase B /RPLC
0
10
20
30
Time (min)

B.

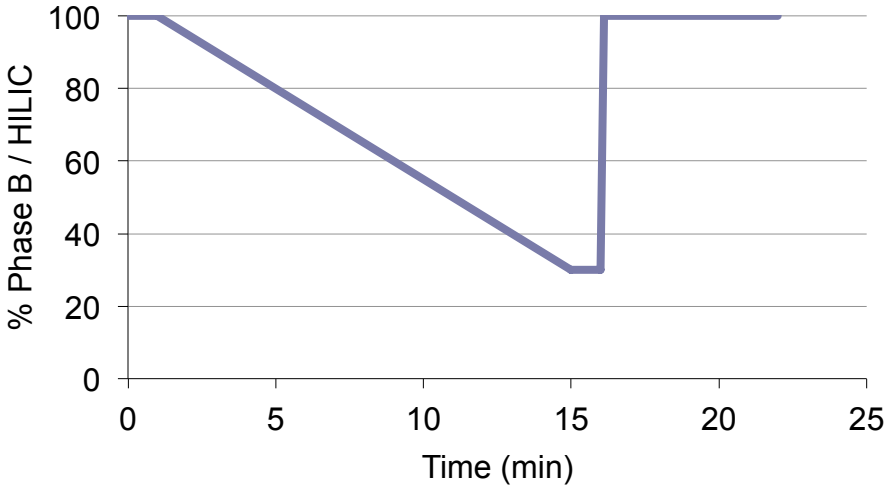
100
80
60
40
20
0
% Phase B / HILIC
0
5
10
15
20
25
Time (min)

Figure S1.

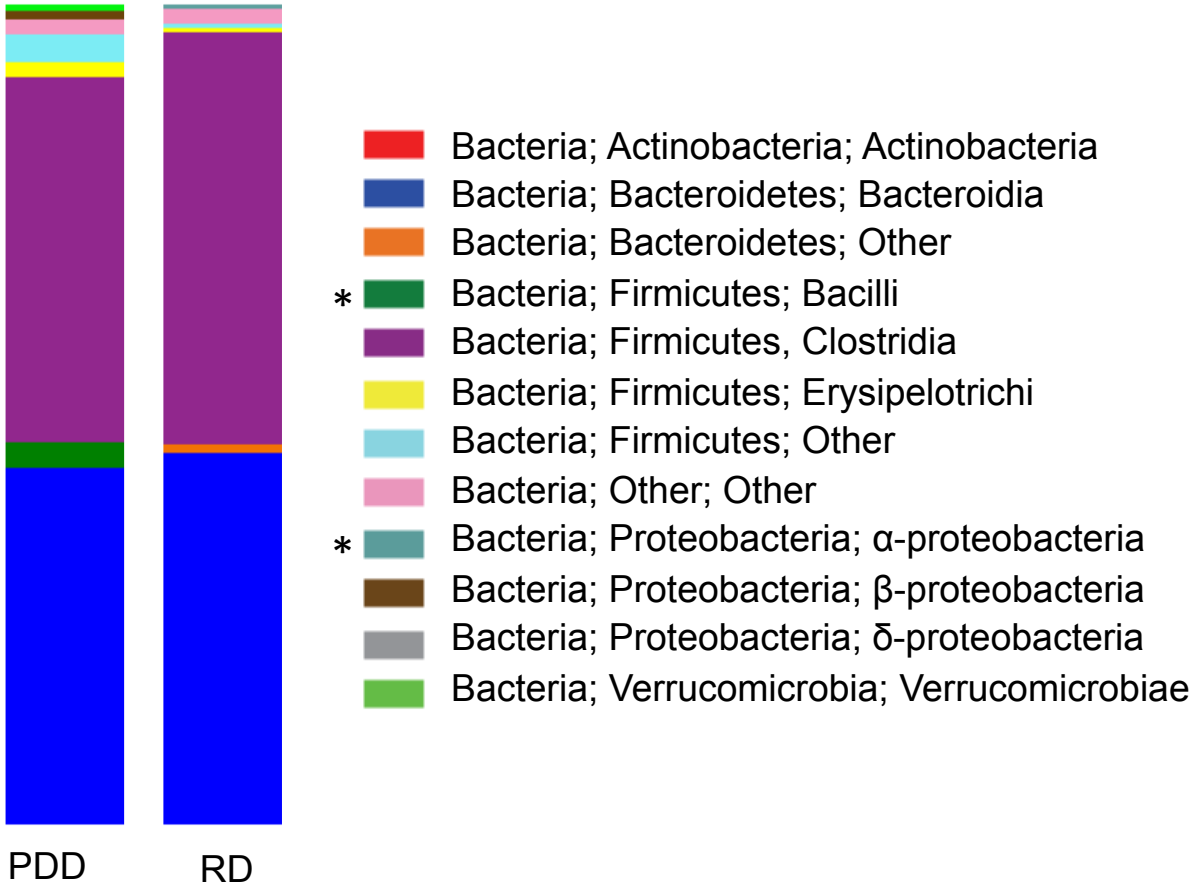
PDD
RD
Bacteria; Actinobacteria; Actinobacteria
Bacteria; Bacteroidetes; Bacteroidia
Bacteria; Bacteroidetes; Other
* Bacteria; Firmicutes; Bacilli
Bacteria; Firmicutes, Clostridia
Bacteria; Firmicutes; Erysipelotrichi
Bacteria; Firmicutes; Other
Bacteria; Other; Other
* Bacteria; Proteobacteria; α-proteobacteria
Bacteria; Proteobacteria; β-proteobacteria
Bacteria; Proteobacteria; δ-proteobacteria
Bacteria; Verrucomicrobia; Verrucomicrobiae

Figure S2.

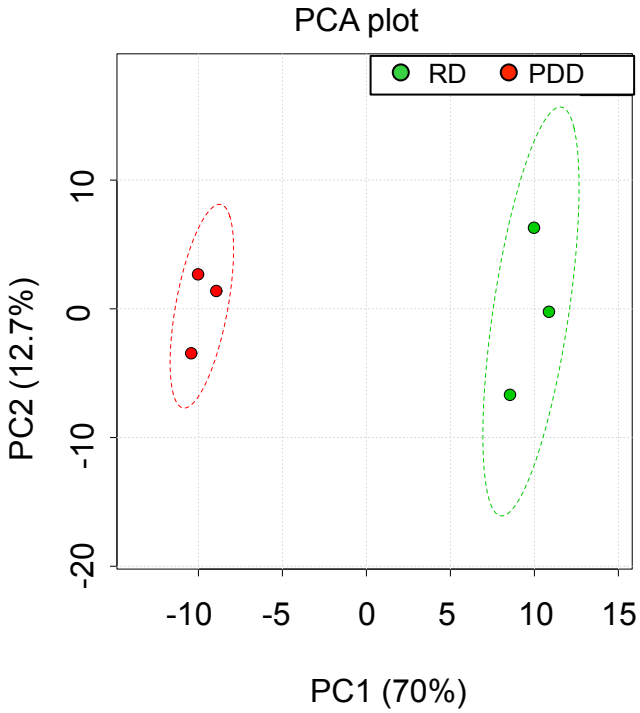

Figure S3.

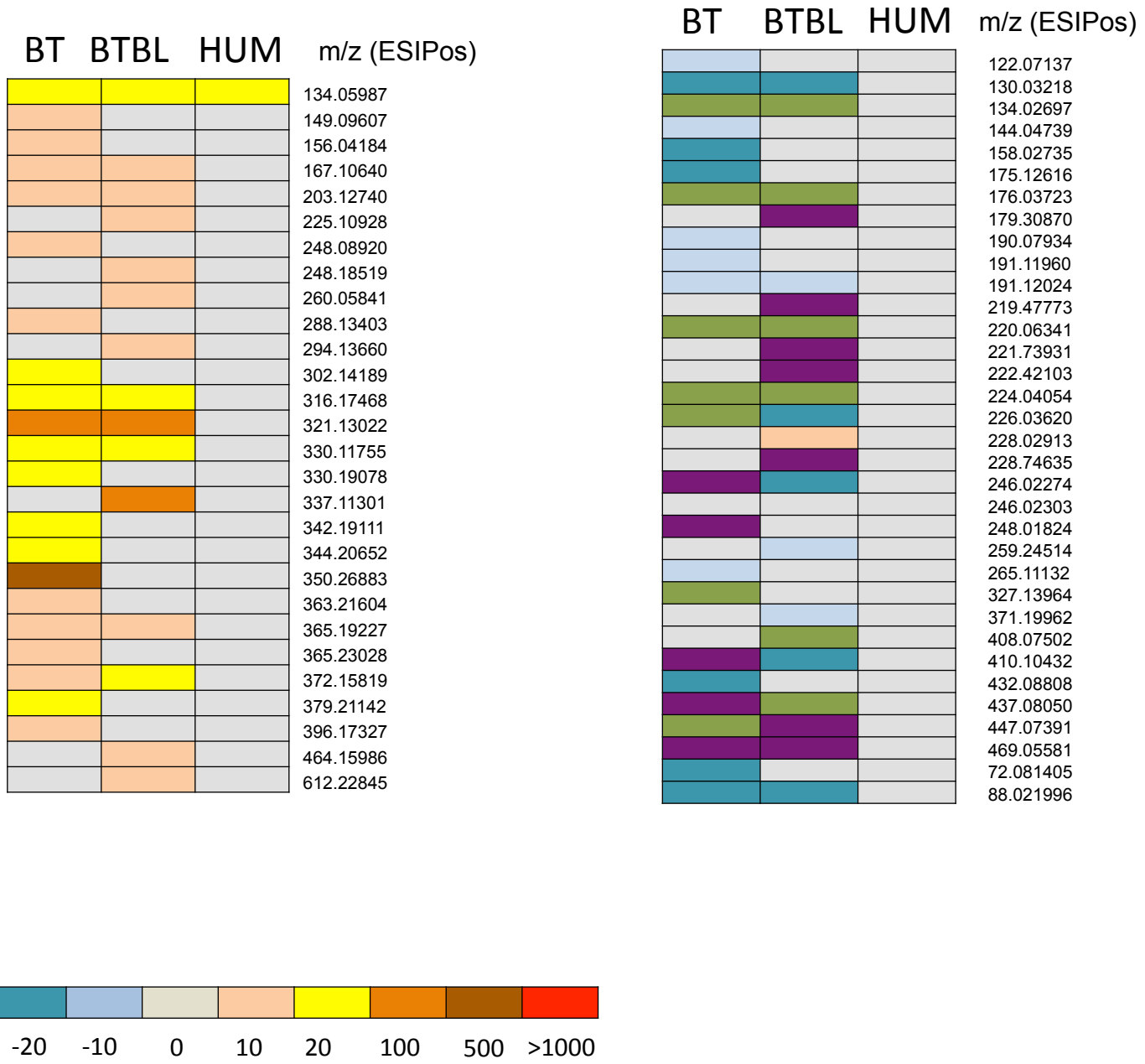
BT BTBL HUM m/z (ESIPos)
134.05987
149.09607
156.04184
167.10640
203.12740
225.10928
248.08920
248.18519
260.05841
288.13403
294.13660
302.14189
316.17468
321.13022
330.11755
330.19078
337.11301
342.19111
344.20652
350.26883
363.21604
365.19227
365.23028
372.15819
379.21142
396.17327
464.15986
612.22845
BT BTBL HUM m/z (ESIPos)
122.07137
130.03218
134.02697
144.04739
158.02735
175.12616
176.03723
179.30870
190.07934
191.11960
191.12024
219.47773
220.06341
221.73931
222.42103
224.04054
226.03620
228.02913
228.74635
246.02274
246.02303
248.01824
259.24514
265.11132
327.13964
371.19962
408.07502
410.10432
432.08808
437.08050
447.07391
469.05581
72.081405
88.021996
Fold Change
<-500
-100
-20
-10
0
10
20
100
500
>1000

Figure S4.

A.

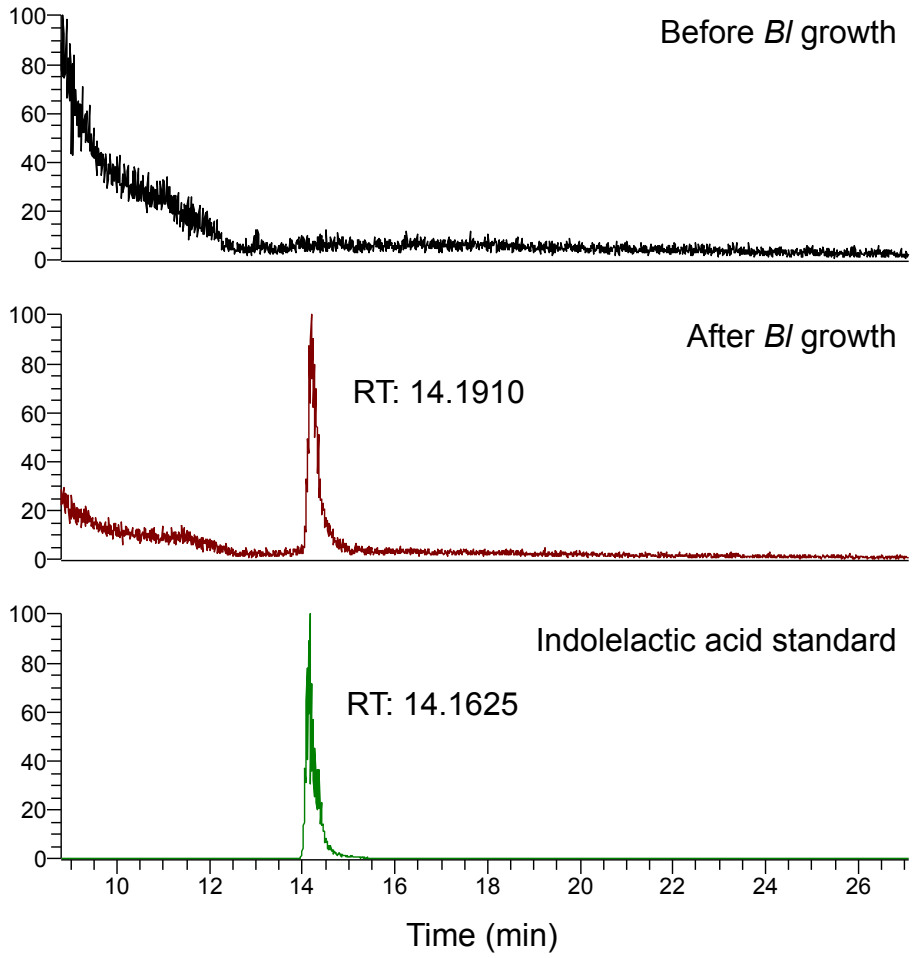
Before *Bl* growth
After *Bl* growth
RT: 14.1910
Indolelactic acid standard
RT: 14.1625
Time (min)

B.

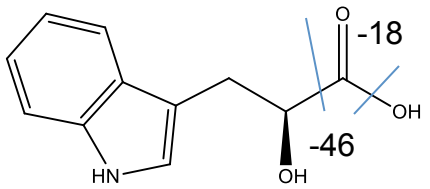
O
-18
OH
-46
HN
OH

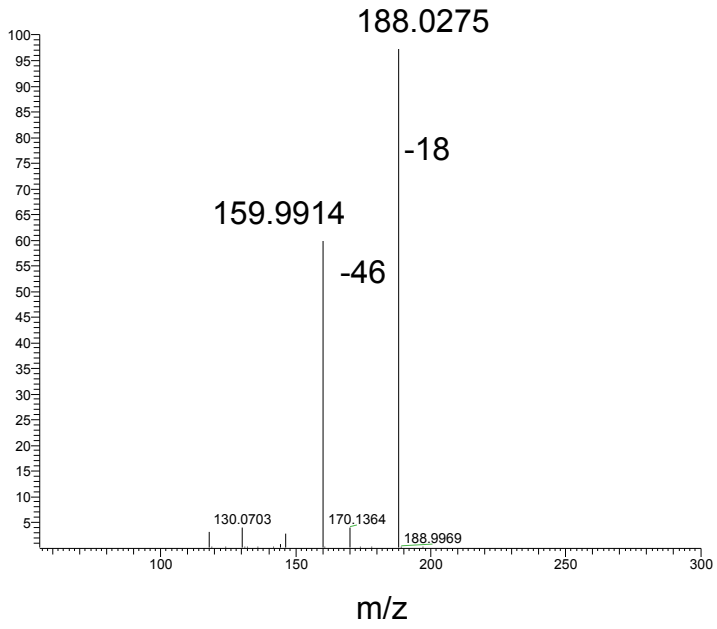
188.0275
-18
159.9914
-46
130.0703
170.1364
188.9969
m/z

Figure S5.

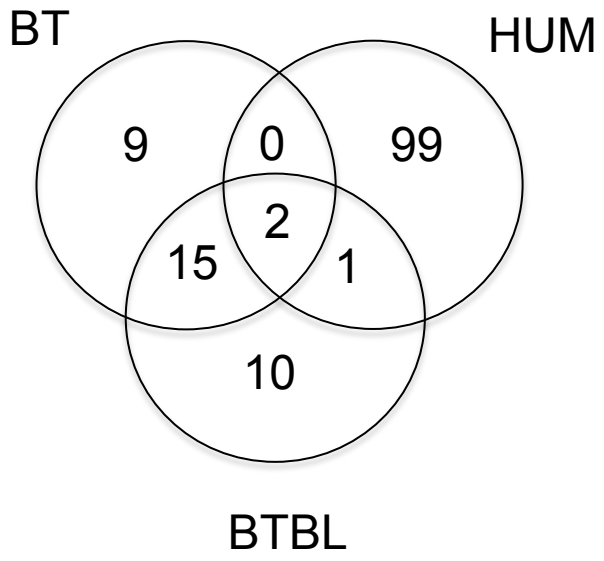

Figure S6.

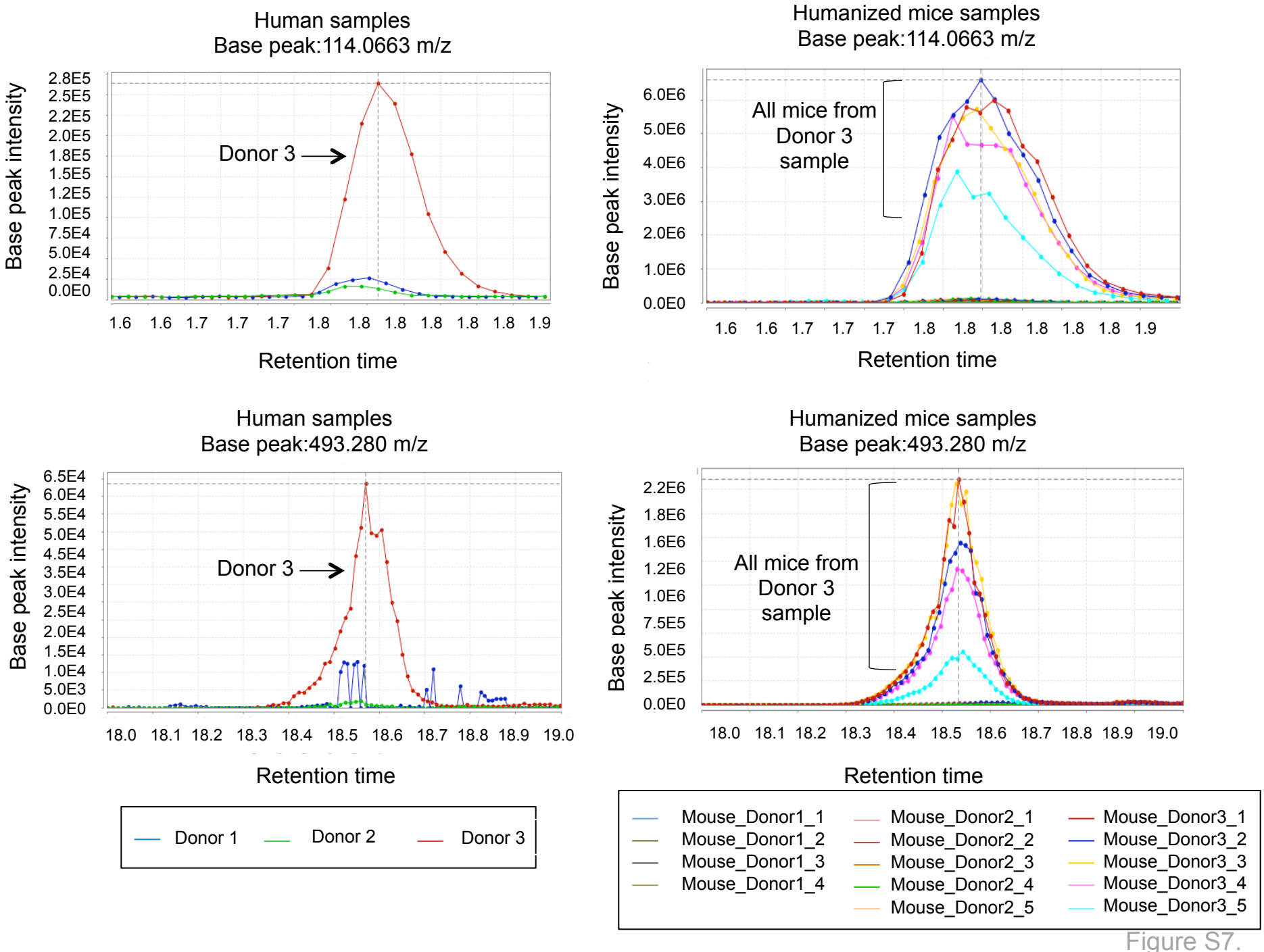
Human samples
Base peak:114.0663 m/z
Base peak intensity
Donor 3
Retention time
Humanized mice samples
Base peak:114.0663 m/z
All mice from Donor 3 sample
Retention time
Human samples
Base peak:493.280 m/z
Base peak intensity
Donor 3
Retention time
Humanized mice samples
Base peak:493.280 m/z
All mice from Donor 3 sample
Retention time
Donor 1
Donor 2
Donor 3
Mouse_Donor1_1
Mouse_Donor1_2
Mouse_Donor1_3
Mouse_Donor1_4
Mouse_Donor2_1
Mouse_Donor2_2
Mouse_Donor2_3
Mouse_Donor2_4
Mouse_Donor2_5
Mouse_Donor3_1
Mouse_Donor3_2
Mouse_Donor3_3
Mouse_Donor3_4
Mouse_Donor3_5

Figure S7.

Exact Mass: 131.0695

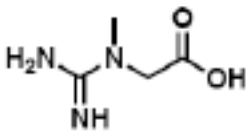

creatine

Exact Mass: 113.0589

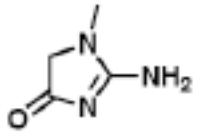

creatinine

Exact Mass: 160.1000

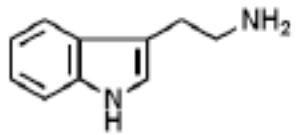

tryptamine

Exact Mass: 133.0528

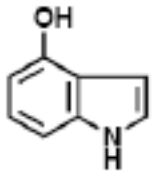

hydroxyindole

Exact Mass: 309.0849

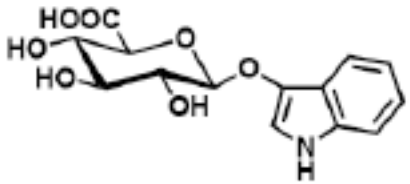

indoxyl glucuronide

Figure S8.